Dupe 71634 5

WORLDWIDE OCEANIC WIND AND WAVE FORECASTS USING A SATELLITE RADAR-RIOMETER

by

Richard K. MOORE
Professor of Electrical Engineering
Director, Remote Sensing Laboratory
The University of Kansas
Lawrence, Kansas, U.S.A.

and

Willard J. Pierson
Professor of Oceanography
Department of Meteorology
& Oceanography
New York University
New York, New York, U.S.A.

SOMMAIRE

L'accroissement de la rétrodiffusion radar qui accompagne les augmentations de vitesse des vents et d'amplitude des vagues constitue un fait connu depuis de nombreuses années. Ce n'est que récemment, toutefois, que les théories ont commencé à apporter des explications satisfaisantes de la diffusion due à la mer.

En outre, les mesures par instruments aéroportés, de la diffusion due aux vitesses de vents élevées sont récentes. L'augmentation du coefficient de diffusion à des longueurs d'ondes centimétriques, avec des vitesses de vents allant jusqu'à 50 noeuds, semble indiquer que l'on peut avoir recours à la mesure du coefficient de diffusion pour déterminer la vitesse du vent. Si l'on peut effectuer ces mesures à partir d'un satellite, on pourra établir la structure globale des vents soufflant à la surface des océans et prédire ainsi les houles des océans du monde entier. L'atténuation des ondes centimétriques peut être compensée par la mesure de la température effective vue par l'antenne radar.

Une théorie quantitative des images radar de l'océan fut d'abord proposée au début des années 50. Cette théorie a été récemment améliorée grâce à la méthode des perturbations, suggérée à l'origine par Rice, et à la méthode de Kirchoff, que Davies fut le premier à utiliser pour la solution de ce problème.

On peut attribuer la plupart des divergences observées autrefois entre la théorie et l'expérience à l'emploi de descriptions de la surface, choisies davantage parce qu'elles se prêtaient à un traitement mathématique que pour leur exactitude.

Malheureusement, il n'existe pas encore de descriptions adéquates de la surface des océans pour les vitesses de vent élevées et les phénomènes à petite échelle, particulièrement importants pour les radars à ondes centimétriques. Toutefois, l'emploi, dans les deux cas de la théorie, d'approximations du spectre de surface des océans a permis d'améliorer, récemment, la description théorique des images océaniques reçues par l'écran radar. L'auteur examine certaines de ces nouvelles méthodes et la comparaison établie entre celles-ci et les résultats expérimentaux.

C'est seulement au cours de ces deux dernières années que l'on a procédé à des mesures des images de l'océan reçues par radar dans le cas de vents soufflant à des vitesses supérieures à 30 noeuds environ (si l'on excepte quelques mesures antérieures effectuées au voisinage du littoral ou à partir de bateaux sous un trés faible angle d'incidence. Des mesures récemment effectuées par le laboratoire de Recherche de la Marine des Etats-Unis et par la NASA ont fourni des informations sur la diffusion, pour des fréquences allant de 0,4 GHz à 13,3 GHz, au dessus de surfaces marines où les vents variaient de moins de 10 noeuds à environ 50 noeuds.

Pour une fréquence de 0,4 GHz, la forme de courbe du coefficient de diffusion varie peu avec la vitesse du vent. Les observations effectuées à la fois par le laboratoire de Recherche Naval pour 9 GHz et par la NASA pour 13,3 GHz révèlent que la diffusion augmente avec la vitesse du vent pour des angles de quelques dizaines de degrés avec la verticale : par contre, les observations relatives à la fréquence de 13,3 GHz indiquent un effet de vent supérieur à celles effectuées pour 9 GHz. Bien qu'il soit possible de rendre la technique expérimentale utilisée en partie responsable de cette différence, celle-ci semble être réelle et montre que l'on devrait, pour mesurer les vents de surface, utiliser des radars à fréquences supérieures à la bande X.

On a proposé un système de mesure des vents à partir de satellite ; ce système permettrait de déterminer les vents sur toute la surface marine du globe, à des intervalles suffisamment fréquents pour établir des prévisions du temps et de l'état des mers à l'intention des marins, pêcheurs et autres usagers de l'océan.

Pour obtenir des résultats optimaux, il faudrait qu'un tel système dépende de mesures absolues, de puissance et utilise des radars capables d'effectuer un bon balayage latéral de la trajectoire du satellite de façon à ce que l'on puisse observer une vaste portion d'océan à chaque passage de ce satellite.

L'emploi d'un récepteur Doppler semblable au radiomètre de Dicke utilisé par les radio-astronomes permettra à un système de ce genre de fonctionner avec une précision satisfaisante, même avec des rapports signal/bruit, approchant de l'unité. Un rapport signal/bruit aussi peu élevé permettra d'utiliser des émetteurs de puissance relativement faible, même à des fréquences supérieures à 10 GHz.

L'utilisation de ces hautes fréquences implique que le signal radar subira une atténuation en traversant d'épais nuages ou de pluie. De récentes mesures effectuées à l'aide des radiomètres à micro-ondes ont montré que l'on peut utiliser la température effective mesurée par le radiomètre (en grande partie déterminée par les radiations émises à partir de la région d'atténuation) pour établir l'atténuation dans l'atmosphère.

L'association d'un radar et d'un radiomètre serait donc plus efficace pour étudier les vents marins qu'un radar seul.

Les données tant théoriques qu'expérimentales obtenues au cours de ces deux dernières années indiquent qu'un concept tel que celui décrit plus haut sera certainement valable pour la mesure des vents si l'on peut établir l'image reçue par l'écran radar sous deux angles d'incidence pour chaque point situé sous le satellite. Un tel système ne pourrait pas couvrir une aussi vaste portion d'océan pour chaque passage du satellite, et donnerait, pour les vitesses de vent observées, un quadrillage moins serré qu'un système faisant appel à des mesures absolues du coefficient de diffusion. La théorie semble indiquer que la technique des mesures absolues peut-être satisfaisante, mais il faut procéder à un complément d'expériences. (Il se peut que l'on dispose des résultats de ces expériences à la date de la réunion).

WORLDWIDE OCEANIC WIND AND WAVE FORECASTS USING A SATELLITE RADAR-RADIOMETER

Richard K. Moore
Professor of Electrical Engineering
Director, Remote Sensing Laboratory
The University of Kansas
Lawrence, Kansas, USA

and

Willard J. Pierson
Professor of Oceanography
Department of Meterology & Oceanography
New York University
New York, New York, USA

SUMMARY

The relationship between radar return from the sea at 2.25 cm wavelength and the speed of the wind disturbing the sea offers an opportunity for a satellite system to provide information for a global wave forecasting system. Results of measurements over seas with surface winds of 12.5 knots to 49 knots presented here indicate that the radar return at angles of incidence in the 25°-40° range increases rapidly with windspeed up to about 25 knots and less rapidly at higher speeds. Comparison of the observations with computations based on application of physical optics to a new composite model of the ocean wave spectrum indicates at least qualitative agreement.

The brightness temperature measured by a microwave radiometer looking at the sea is also proportional to wind speed, but the effect of atmospheric attenuation is much greater on brightness calibration for the radar scatterometer is suggested. A proposed instrument uses a scanning antenna and a common receiver for the radar and radiometer.

An example of the benefits to be gained by using the more plentiful satellite observations of wind speed is presented for the South Atlantic. Because of the sensitivity of both the radar return and the wave spectrum to wind direction, other information, such as that gained from satellite cloud photographs, must be used to perform the forecasts, and the radar data cannot be used alone.

INTRODUCTION

Forecasts of ocean wave spectra permit optimum routing of ships to allow greater speed and prevent storm damage. These forecasts, and meteorological forecasts, depend on knowledge of the surface wind field over the oceans. The relationship between radar backscattering and the winds permits global wind monitoring from a satellite, provided proper wavelengths are chosen and cloud attenuation is small. Combining a microwave radiometer with the radar scatterometer allows use of the greater sensitivity of the radiometer to cloud attenuation for removing most of the effect of attenuation of the backscatter signal.

Forecasting ocean wave spectra requires knowledge of the wind field over a large area and long time. Waves can propagate to long distances, and the effect local winds remains long after the winds have ceased. Numerical forecasting depends upon iterative solution of the appropriate equations over a period of about a week prior to the forecast time. Updating at about 6 hour intervals permits continuous extension of the forecast. A 120 km point spacing is used for forecasting, since a finer grid would require too much computer storage and time. This widely spaced grid permits use of a satellite instrument with resolution of 10s of km, which makes design simpler for the instrument.

Radar observations of backscatter from the sea have been made for nearly 30 years, but recent measurements from aircraft flying to stormy areas in the North Atlantic have permitted significant improvement in the available information. The data presented here were obtained by aircraft of the U. S. National Aeronautics and Space Administration (NASA) in March of 1968 and 1969. We had hoped to present data from flights in February of 1970, but data reduction is not yet complete. The 1968 data were only at 13.3 GHz (2.25 cm) with vertical polarization, and the 1969 data are from the same system plus a multipolarization 0.4 GHz (75 cm) system. The experimental results at 13.3 GHz are compared with theoretical computations based on a new composite wave spectrum.

A scanning radar-radiometer is proposed as an operational system for space. The radar will operate in an ICW mode, permitting use of low signal-to-noise ratio and radiometer-like calibration. Although both systems may use the same receiver, the radar bandwidth is smaller, as optimum S/N occurs when radar bandwidth is equal Doppler bandwidth of the signal.

A sample integration of satellite data into a forecast is presented to illustrate the major advantages of the satellite system.

RADAR BACKSCATTER OBSERVATIONS

Most previous measurements of radar backscatter were (1) near grazing incidence, or (2) near coastlines, or (3) without adequate information on the ocean conditions. Apparently the NASA measurements and U. S. Naval Research Laboratory (NRL) measurements within the last two years are the first to overcome these restrictions. The NRL measurements are reported elsewhere.[1] Here we report primarily on the NASA measurements.

Various observers have indicated some sort of "saturation" in the increase of radar return with windspeed, and Wright[2] has predicted this saturation on the basis of a perturbation theory for radar scatter and the Phillips expression for the "high-frequency tail" of the ocean wave spectrum. Apparently the validity of Wright's approach depends on the wavelength of the radar, for the measurements reported here show no saturation for 2.25 cm radar up to about 50 knots windspeed, whereas saturation does occur in our 75 cm measurements. NRL's 3.3 cm measurements show much smaller variation with windspeed than found at 2.25 cm.

THE RADAR SCATTEROMETER

The radar scatterometer used for the measurements reported here has a fan beam directed along the flight path of the aircraft, as shown in Slide 1. Returns from different angles within this beam are separated by filtering the appropriate Doppler frequencies. Isodops for horizontal flight are hyperbolas as shown on the slide, so a filter of width Δf_d can separate all returns between θ_1 and θ_2.[3]

Slide 2 shows a block diagram of the simple CW-Doppler radar system used. A klystron transmitter also provides a local oscillator signal, so the receiver is a homodyne. The Doppler frequencies received are amplified in an audio amplifier, and the results recorded on magnetic tape. On the ground the tape may be spectrum-analyzed either in analog or digital fashion. Two channels are used in quadrature to provide the phase information required to separate positive and negative Doppler frequencies. A calibration signal

was inserted with a ferrite modulator driven by an audio frequency outside the Doppler frequency band. Since the output of this calibrator is proportional to the transmitted signal, and since it passes through the same receiver/recorder channel as the received signal, it can provide an accurate calibration. Unfortunately, the ferrite modulator is somewhat temperature sensitive and subject to remanent-magnetism errors, so an uncertainty of about ±3 dB occurs in the absolute level of the signal. A calibrate source using PIN diodes and modulation at a different level was used in the 1970 flights, so the absolute calibration should be better for these data when they become available.

13.3 GHz SACTTEROMETER DATA

Because of the potential errors in absolute level, the data were normalized by presenting the ratio of differential scattering coefficient at any incident angle to that at 10°. Slide 3 shows a representative group of observations normalized in this fashion. Clearly the 49 knot upwind return is much higher than the cross-wind return for the same wind speed, as would be expected. Comparable results were also found at lower wind speeds down to the 12.5 knot level, where little difference can be seen.

Slide 4 shows a more extensive set of observations for the upwind condition. The increase in normalized radar return with windspeed is evident, although some other effect must also be present to cause the difference between the 12.5 and 13 knot curves. Repeatability between the two years was amazingly good in the 20-30 knot range, where most data were available. Other curves are not shown here because they are so like the ones shown and would make the graph hard to interpret.

Recently an error was found in the antenna pattern used in the data reduction, so some changes in shape of the curves will result when the reprocessed data are available. Nevertheless, the separation between curves for different wind speeds will remain exactly the same. For data presented in this way the only change that would affect the relative postions of the curves would be a drift in the amplitude-vs-frequency characteristic of the audio amplifier, and this is certainly a very stable characteristic--as shown by the remarkable agreement between data taken a year apart.

For windspeed measurement, the observations should be plotted vs windspeed at a fixed angle. Slide 5 shows this. Although the variation at 15° is not significant, variation with windspeed at both 25° and 35° is quite strong. For the upwind case, the scattering at 35° varies as $v^{2.85}$ below 25.5 knots as as $v^{2.15}$ above 25.5 knots (v is windspeed). For the cross wind case, the scattering at 35° varies only linearly with v above 25.5 knots. With measurements of sufficient accuracy, this should permit windspeed determination over this range of speeds, provided the direction is known from other information.

0.4 GHz SCATTEROMETER DATA

The 0.4 GHz scatterometer also uses the fan-beam Doppler technique, but uses a superheterodyne rather than a homodyne receiver. Absolute accuracy should be better with this system than at 13.3 GHz. Slide 6 shows the vertically polarized observations with this system, compared with similar observation by NRL. All wind speeds give nearly the same results, although both the NASA and the NRL data show a slight tendency for the signal to be lower at 49 knots than at 12 knots. Slide 7 shows the horizontally polarized observations, and the same conclusions can be drawn. Because of this lack of sensitivity to wind speed, this frequency is not likely to be useful for wing measurement.

THEORY AND EXPERIMENT

Various theories have been used to describe the radar backscatter from the ocean. Geometric optics, of facet theories have been used in the past. Wright[2], Fung[4], and a group of Russian authors[5] have used perturbation techniques. Others have used physical optics, based on the Kirchhoff approximation that the field on the surface is the same as it would be for an infinite plane tangent to the surface at that point. Perturbation techniques alone give amazingly good results when considered in light of the breakdown of the approximation involved for any surface-height variation of the order of $\lambda/2\Pi$, but we do not believe the first-order perturbation can possibly give a true description of scatter from the open ocean. On the other hand, the fact that this method works at all indicates that the phenomenon causing return from the ocean must be strongly influenced by the very smallest waves, and that Bragg scatter from these small waves is significant.

The key point in any theory is the surface description used. The theoretical results presented here are based on application of physical optics to a new wave-spectrum model. The elements of this model are given in Slide 8. Region 1 is the now-standard Pierson-Moskowitz model, which gives a good description of large-scale structure on the fully-developed sea. In the high frequency limit this model, like that due to Phillips, is assymptotic to k^{-3}. Region 2 is associated with dynamic equilibrium between wind and waves. In this region the spectrum is proportional to wind speed v and to $k^{-2.5}$. The transition between Regions 1 and 2 is at a frequency (or k) that must be determined somewhat arbitrarily on the basis of experiment; the appropriate parameter is Υ. Region 3 involves capillary (surface tension) waves, which are much smaller than the gravity waves of Region 1. In this region, however, the shape of the spectrum is the same as that for the high-frequency gravity waves, but the amplitude is about 8 times as great. The 4th region is the viscosity range, and is unimportant to this discussion.

Apparently the significant size of structures on the ocean for a radar of 2.25 cm wavelength are those associated with Regions 2 and 3, depending somewhat on the wind speed. Certainly these sizes are the same order of magnitude as those required for Bragg scattering of such radar frequencies. Chia[6] originally applied the Pierson-Moskowitz spectrum and physical optics to the long-crested case; he obtained results (assuming unit reflection coefficient) much like those shown in Slide 9. With this spectrum there is little effect of wind speed on the backscattering. Chia also applied a spectrum like that of Region 2 and showed considerable variation with windspeed, but his curves were the wrong shape. Now we have applied the entire spectrum of Regions 1, 2, and 3, obtaining the results shown in Slide 10. Although this was a crude attempt (unity reflection coefficient and long-crested waves), it clearly is in general accord with the experimental observations previously shown.

The comparison between this theory and experiment is illustrated in Slide 11. Because of uncertainties in absolute levels, the data have been normalized so that all points coincide for 25 knots. With this approach, the crude theory seems to fit the crosswind data quite well. The increase with windspeed for the upwind data is more rapid than the theory indicates. Since γ was selected somewhat arbitrarily for this set of theoretical curves, the agreement is surprisingly good. Work is now in progress to extend the calculations for short-crested waves and for the reflection coefficients appropriate to the cases of vertical and horizontal polarization.

THE MICROWAVE RADIOMETER

Several investigators have recently shown that a microwave radiometer, although highly sensitive to cloud attenuation, is also sensitive to winds at sea. This result is not surprising, since the microwave radiometer obtains much of its signal by scatter from the surface of the ocean. Fung and Ulaby[7] have recently developed a theory thst explains the observations near vertical incidence much better than the earlier theory of Stogryn[8]. The principal difference between the theories is that Stogryn used a Gaussian autocorrelation function of surface heights in the physical optics computation of scatter, whereas Fung and Ulaby used an exponential. Slide 12 shows the comparison of the two theories with some observations by Nordberg of NASA/Goddard Space Flight Center.

Because of the sensitivity of the radiometer to the atmosphere, the system proposed here uses it to calibrate the scatterometer, even though it could be used for windspeed measurement in its own right if the atmosphere were absent. A relatively small increase in attenuation causes a quite large increase in radiometer brightness temperature. Wilson (Slide 13) has shown how this can be used to calculate the atmospheric attenuation causing the increase in brightness, using an upward-looking radiometer. For attenuations below about 8 dB, this method appears quite attractive.

SPACECRAFT SYSTEM

A spacecraft wind-measuring system should cover as much ocean surface as possible in each orbit; accordingly a side-to-side scan seems appropriate. Because of the uncertainties in the absolute calibration of the NASA data a system that uses only one angle is still conjectural, but a system that measures the scattering cross-section at two angles seems guaranteed of success.

Slide 14 shows a system permitting measurements at two angles. The spacecraft radiates at 10° and 35° incident angles, using either a fan beam or two pencil beams. The time of travel between the two positions shown for the spacecraft is only a few minutes or less, so the ocean conditions remain statistically the same. Hence the spacecraft measures the scatter at 10° in its second position for the same ocean area from which the 35° measurement was made at its first position. By correlating these measurements, the wind speed at the surface may be determined, but only along the sub-satellite track.

If further measurements show, as we expect, that data are required from only a single angle to establish the wind speed, a scan like that in Slide 15 can be used. In this scan, the antenna uses a pencil beam that moves from side-to-side of the spacecraft in a plane tilted somewhat ahead of the nadir. With this method the angle of incidence can be kept within the region of maximum variability with sea state. A scan for a 1000 km orbit can readily be 1200 km long, thus providing 11 points at 120 km intervals for the forecasting computer.

Slide 16 shows a sample set of incident angles for 1000 km height of the satellite. Ordinarily the scan would be kept within about 600 km of the ground track; so that, for a 25° tilt of the antenna, the incident angle remains within the 30-40° range.

RADIO-RADIOMETER SYSTEM

The radar scatterometer using a narrow beam antenna like that shown in Slide 15 can be operated in a nearly-CW mode. Because of the difficulty with isolation, the signal is transmitted only until the first return signal appears, and then is turned off during the receiving period. This near-CW operation permits use of a narrow-band receiver, since the harmonics of the long-pulse fundamental rate are insignificant compared with the Doppler frequency spread. Thus, the band width of the receiver is determined by the Doppler spread, which is of the order of kiloHertz for practical cases.

Slide 17 illustrates how the post-detection signal-to-noise ratio can be made high with low predetection S/N by operating the scatterometer much like a radiometer/radio-telescope receiver.[9] Integrating a large enough number of independent samples of signal + noise and a like (or greater) number of noise samples reduces the variance of each so that very small differences can be measured reliably. The equation on the slide shows the signal-to-noise ratio improvement possible with this system. The number of independent samples r is approximately twice the time-bandwidth product of the receiver. With this method signal-to-noise ratio of unity or less at the input may be used successfully in a space system, and the result is a peak power requirement of the order of 10-50 watts, with average power of 2-10 watts.

The radar and radiometer systems may share time or may operate at slightly different frequencies within the capabilities of the antenna and pre-amplifiers. A simplified version of the block diagram of such a system is shown in Slide 18. An actual system would probably use more switches to provide the calibration signal for the radiometer, and would contain a provision to pass an attenuated version of the transmitter output through the receiver to calibrate the scatterometer. The Dicke switch in the radiometer alternately connects the radiometer receiver to the hot load (at accurately known temperature) and the antenna, with calibration by switching to a cold load at less frequent intervals. The scatterometer needs no such switch, since its noise calibration is provided by simply recording the output during a time when no scattered signal is present. The noise for the scatterometer is the signal + noise for the radiometer.

APPLICATION TO FORECASTING

The output of a side-to-side scanning system like that proposed will average about 2,500 pairs of $\sigma°$ and T_b per orbit, if only data over ocean are counted. Forecasts are normally made on a 6-hour repetition period, and present data used for the purpose consist of ship reports radioed into meteorological centers at either 6 or 12 hour intervals and cloud information from weather satellites. Enough ship reports to permit adequate forecasts are present only in heavy shipping lanes such as those from North America to Europe. Even in these areas the forecasts often fail because insufficient information is available on storms moving in from regions having little shipping. Hence, this input of over 30,000 data points per day can have a major impact on forecasting weather and waves.[10]

Since the data must be combined with wind direction information to provide accurate reports of surface wind speeds, the operational system will need a combination of updating past weather reports and forecasts on an iterative basis with use of the available ship reports and of cloud photographs from satellites.

Another problem that must be overcome is the use of non-synoptic data. Forecasting presently is based on measurements made by all ships and coastal stations at the same time. The satellite, on the other hand, provides coverage in a continuous strip. The NIMBUS satellite always collects data at local noon or or midnight.

Computer programs to solve both the non-synopticity problem and the wind direction problem are presently being developed at New York University.

An example of the kind of analysis that might result from use of such a system is illustrated with Slide 19 and Slide 20. In Slide 19 a portion of an actual surface analysis for the South Atlantic area is shown. The dots indicate locations of reporting ships and shore weather stations, and the remainder of the analysis is based on combining these data with satellite cloud photographs. Note the high in the upper left and the two lows. Slide 20 shows a hypothetical set of observations from a satellite pass across this region, with the resulting modification to the pressure patterns shown. These changes in size and intensity of the main features of the pattern are quite reasonable to expect with the improved data coverage to be obtained using the satellite.

CONCLUSIONS

The use of a combined radiometer-scatterometer in a satellite to provide surface wind information on a global scale over the oceans has been shown feasible, based on observations of radar sea return at 2.25 cm and of the success of use of radiometers to estimate attenuation through clouds. Reasonably good agreement has been shown between backscatter observations at sea and predictions of a simplified theory based on a long-crested (one-dimensional) 4-part wave spectrum applied to a perfectly-reflecting physical optics formulation of the radar scatter problem.

Additional measurements are under way with a Doppler radar scatterometer operated by NASA Manned Spacecraft Center, and observations of frequency dependence of the ocean backscatter are planned with a radar-radiometer to be used by NASA/Langley Research Center. A radar-radiometer will probably be tested in space in 1972 on the Skylab to be flown by NASA.

This work was supported by the U.S. Naval Oceanographic Office under contract N62306-67-C-0044 and by NASA/MSC under contract NAS9-10261 with The University of Kansas and by the U.S. Naval Oceanographic Office under contract N62306-70-A-0075 with New York University.

REFERENCES

1. Guinard, N. W. and J. C. Daley, "An Experimental Study of a Sea Clutter Model," Proc. IEEE, vol. 58, pp. 543-550, April, 1970.
2. Wright, J. W., "A New Model for Sea Clutter," Transactions of the IEEE, vol. AP-16, pp. 217-223, 1968.
3. Moore, R. K., "Ground Echo," Chapter 25 in Skolnik, M., Radar Handbook, McGraw-Hill Book Company, Inc., New York, pp. 25-20, 25-21, 1970.
4. Fung, A. K. and H. L. Chan, "Backscattering of Waves by Composite Rough Surfaces," Transactions of the IEEE, vol. AP-17, pp. 590-597, 1969.
5. Bass, F. G., I. M. Fuks, A. I. Kalmykov, I. E. Ostrovsky, and A. D. Rosenberg, "Very High Frequency Radiowave Scattering by a Disturbed Sea Surface," Transactions of the IEEE, vol. AP-16, pp. 554-568, 1968.
6. Chia, R. C., "The Theory of Radar Scatter from the Ocean," Ph.D. Dissertation, The University of Kansas, 1968. Also published as Technical Report 112-1, CRES, University of Kansas, October, 1968.
7. Ulaby, F. T. and A. K. Fung, "Effects of Roughness on Emissivity of Natural Surfaces in the Microwave Region," 1970 Southwest IEEE Conference (SWIEEECO), CRES Reprint 133-8.
8. Stogryn, A., "The Apparent Temperature of the Sea at Microwave Frequencies," IRE Transactions Antennas and Propagation, vol. Ap-15, pp. 278-286, March, 1967.
9. Moore, R. K. and F. T. Ulaby, "The Radar Radiometer," Proceedings of the IEEE, vol. 57, pp. 587-590, 1969.
10. Pierson, W. J., L. J. Tick, and L. Baer, "Computer Based Procedures for Preparing Global Wave Forecasts and Wind Field Analyses Capable of using Wave Data Obtained by a Spacecraft," Sixth Symposium Naval Hydrodynamics, ONR Department of the Navy, ACR-136, 1966.

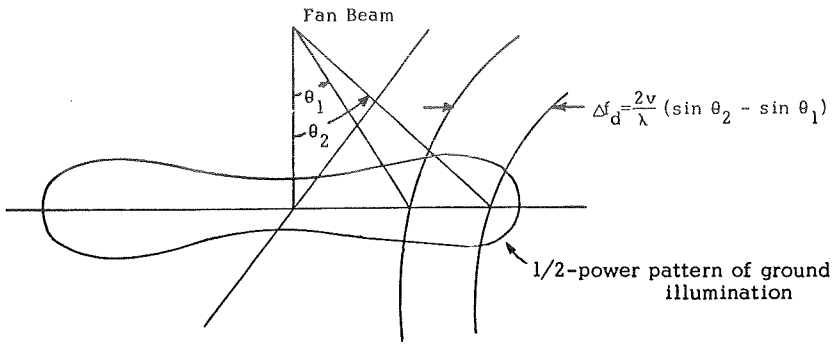

Fig.1 Operation of a fan-beam CW-Doppler scatterometer

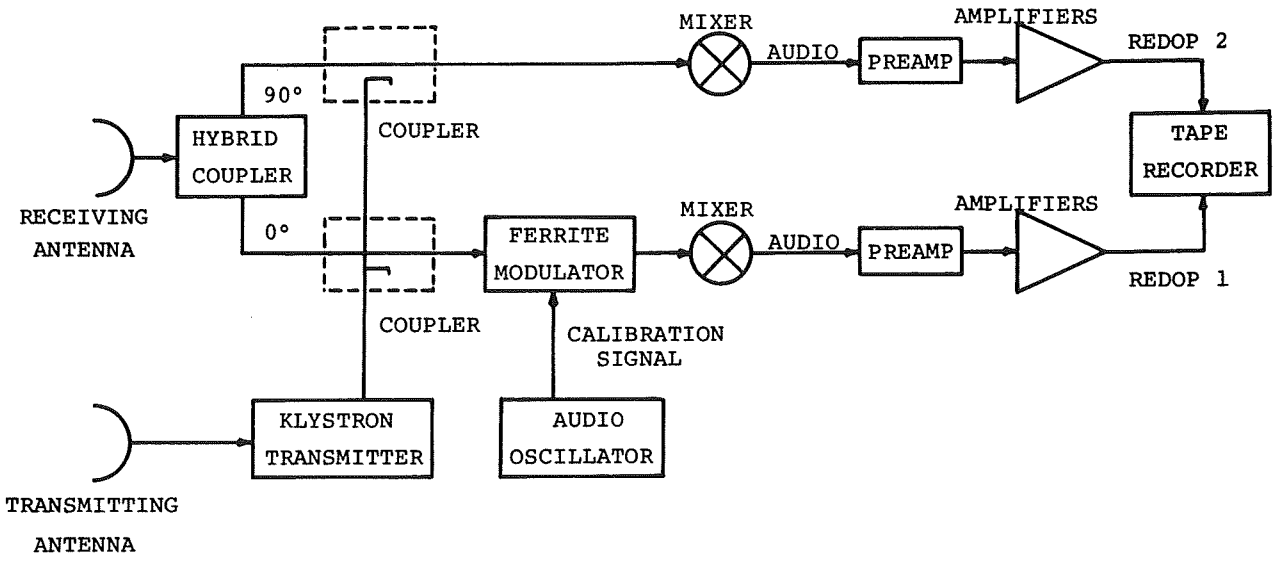

Fig.2 13,3 GHz radar scatterometer block diagram

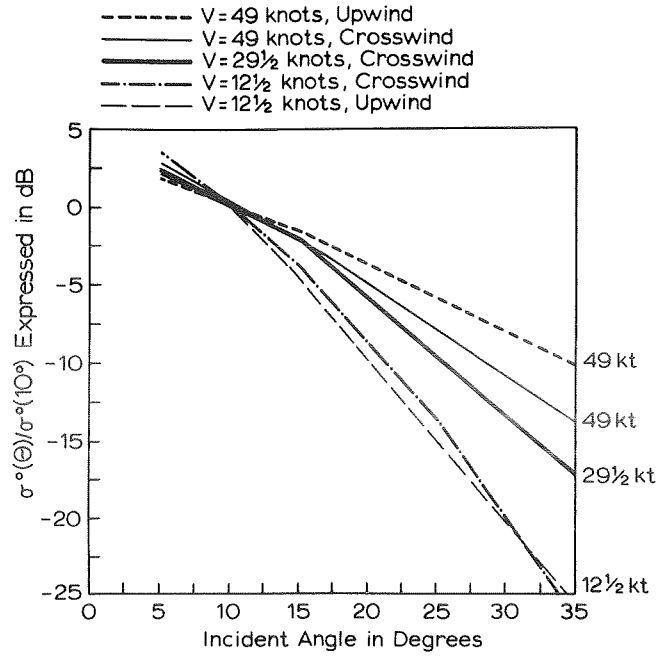

Fig.3 Comparison of crosswind and upwind normalized scattering coefficients at 2.25 cm wavelength, (March 1969 data)

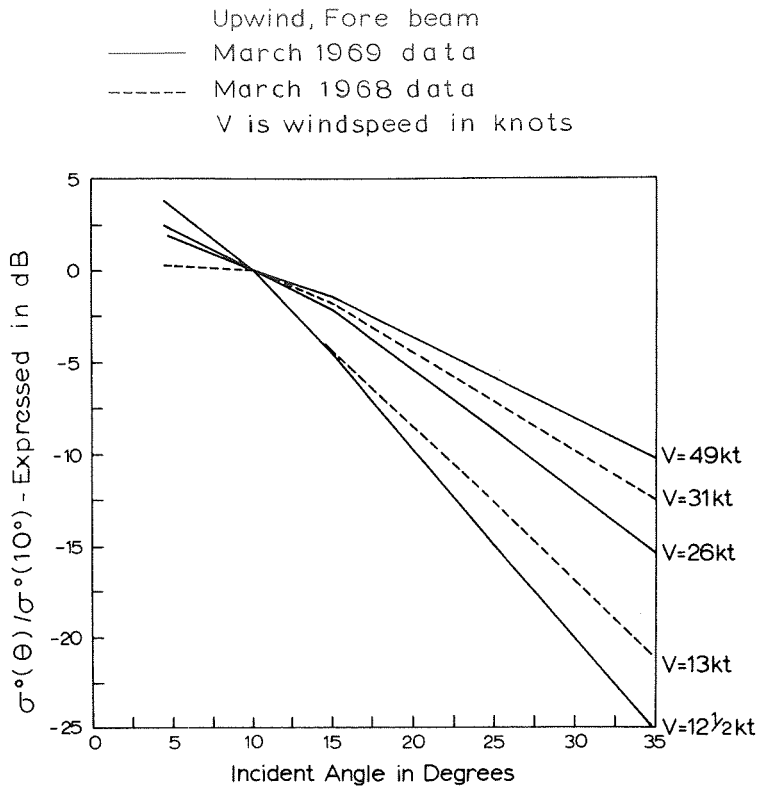

Fig.4 Differential scattering coefficient of ocean at 2.25 cm wavelength normalized to Odb at 10^0

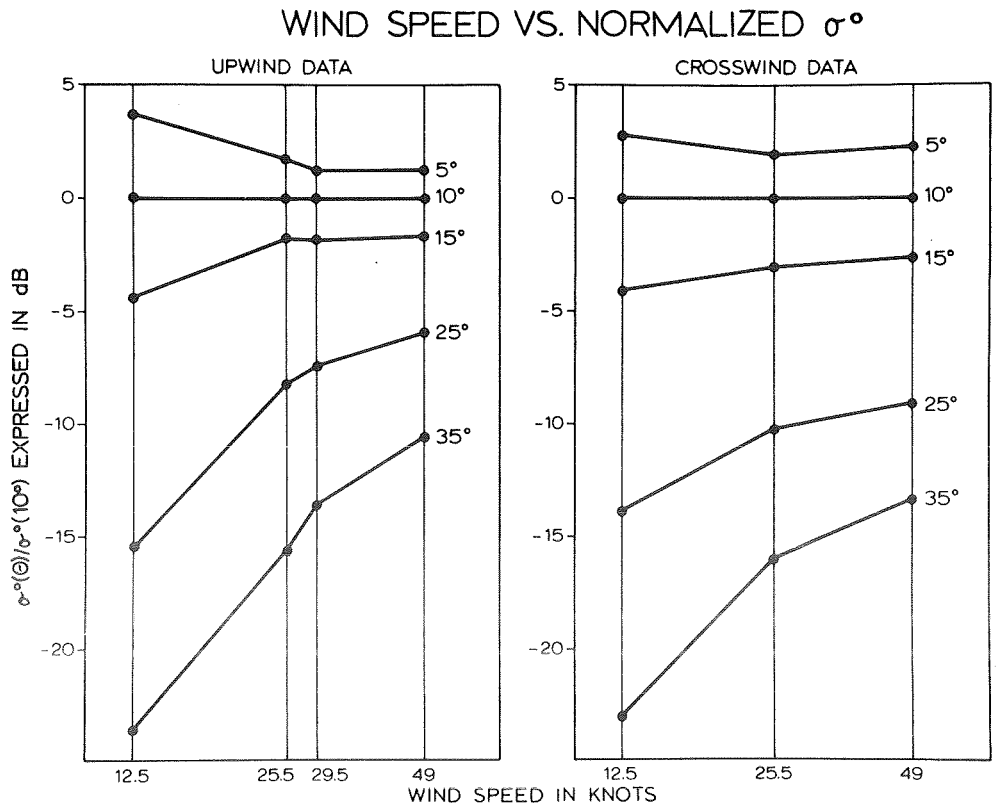

Fig.5 Normalized radar scattering coefficient vs. wind speed and direction at 13.3 GHz. (2.25 cm wavelength)

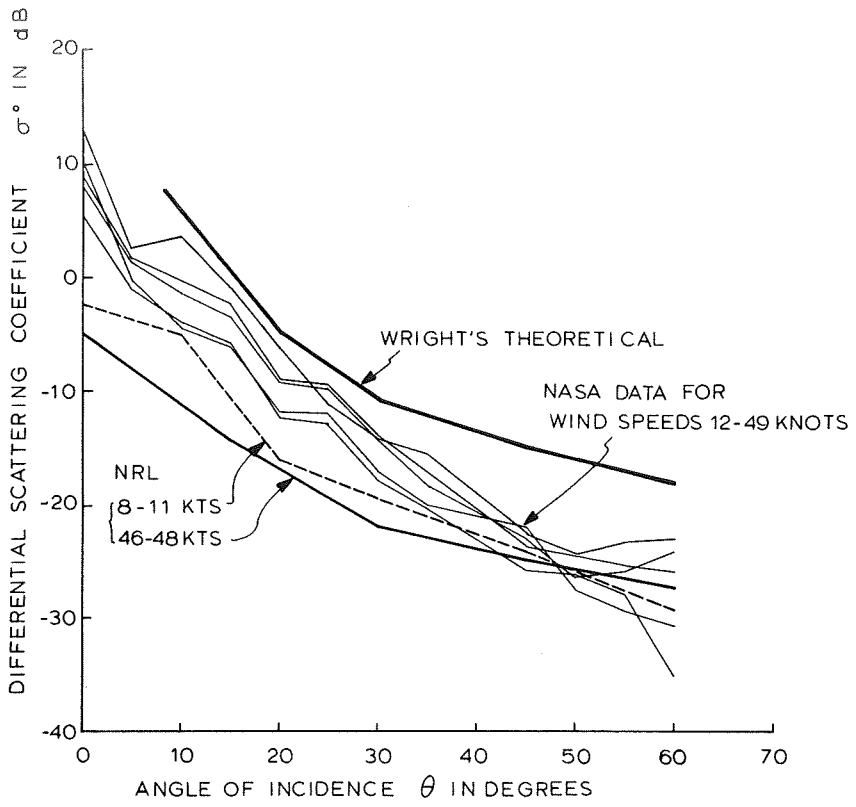

Fig.6 Vertically-polarized 400 MHz radar back-scatter from the ocean

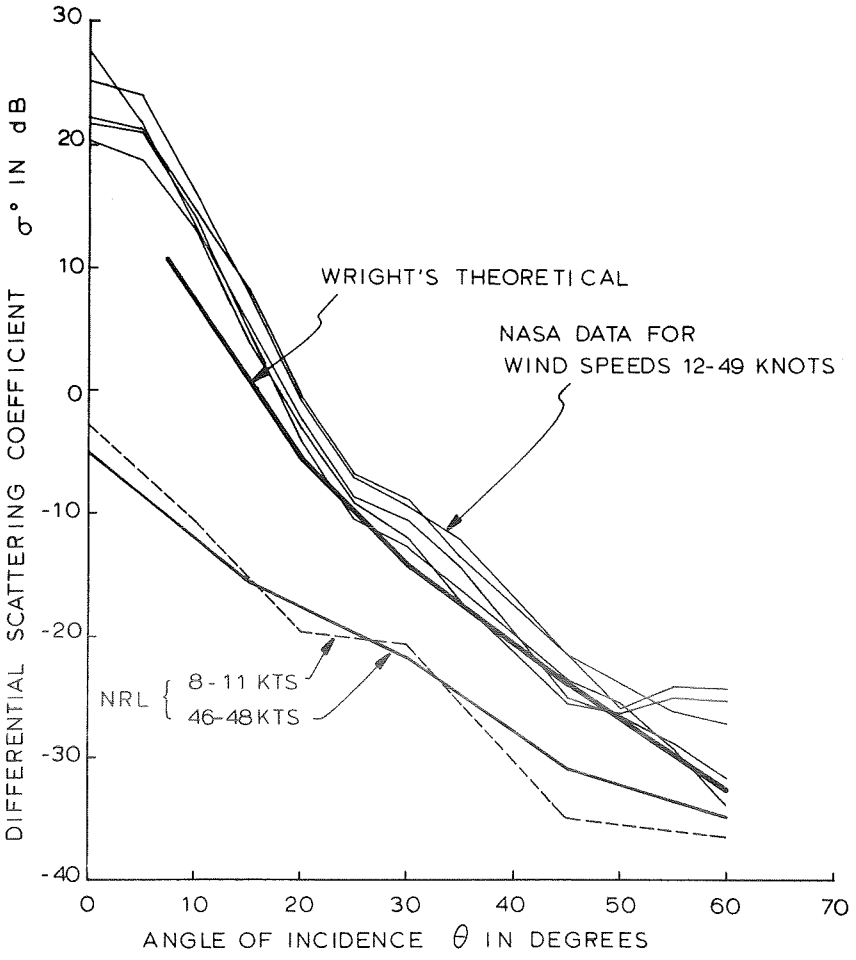

Fig.7 Horizontally-polarized 400 MHz radar back-scatter from the ocean

REGION 1 - SMALL K - PIERSON-MOSKOWITZ FORM ASYMPTOTIC TO AK^{-3}

REGION 2 - INTERMEDIATE K - DYNAMIC EQUILIBRIUM RANGE ASYMPTOTIC TO $BVK^{-2.5}$
TRANSITION REGION 2 - REGION 2 AT $\omega = \frac{\gamma g}{V}$

V = WIND VELOCITY
g = GRAVITATIONAL ACCELERATION
γ = PARAMETER TO BE SELECTED

REGION 3 - CAPILLARY WAVES SPECTRUM $8AK^{-3}$

REGION 4 - VISCOSITY RANGE (MILLIMETER WAVELENGTHS)

Fig.8 Composite wave spectrum

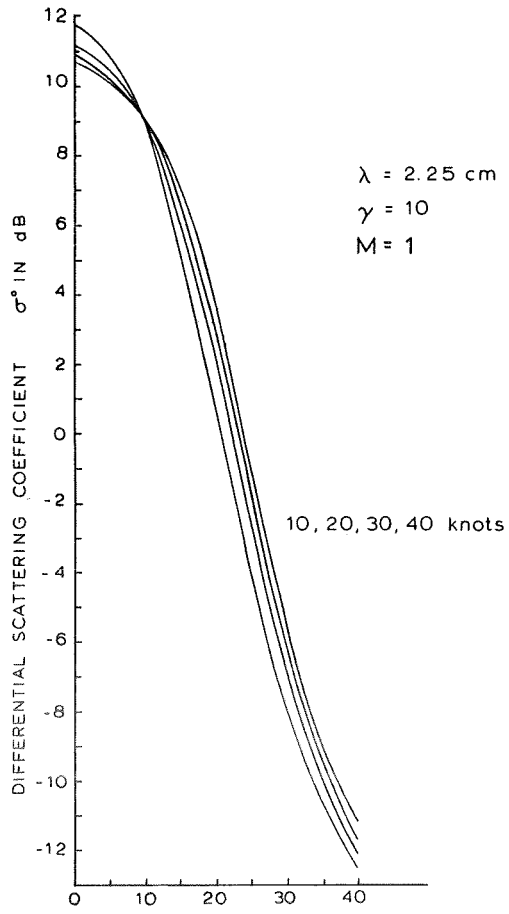

Fig.9 Angle of incidence θ in degrees
Differential scattering coefficient from physical optics (Kirchhoff approximation) Pierson-Moskowitz spectrum (asymptotic to Phillips theory) (long crested waves)

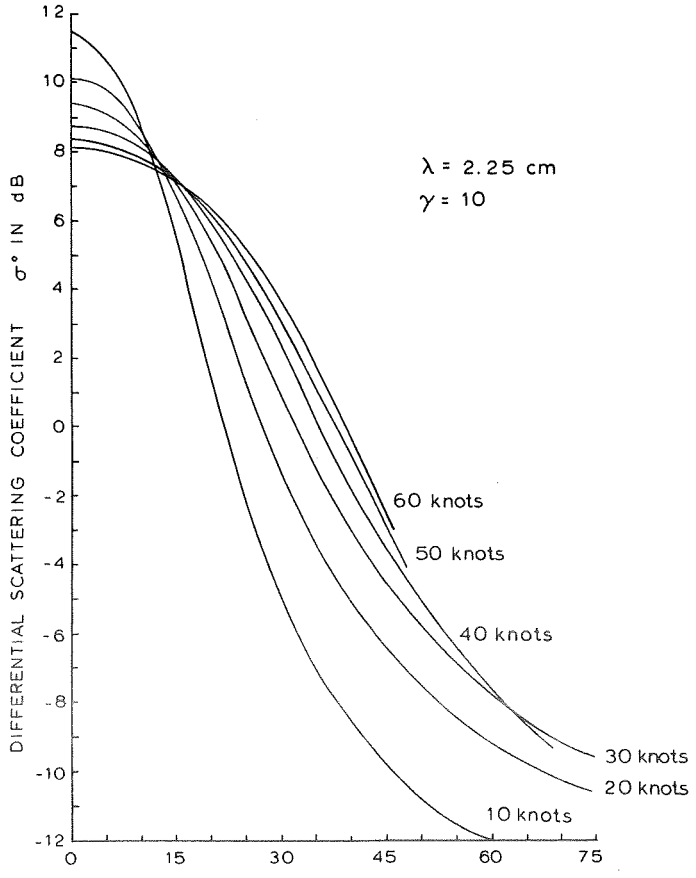

Fig.10 Angle of incidence θ in degrees
Differential scattering coefficient from physical optics (Kirchhoff approximation) composite spectrum (long crested waves)

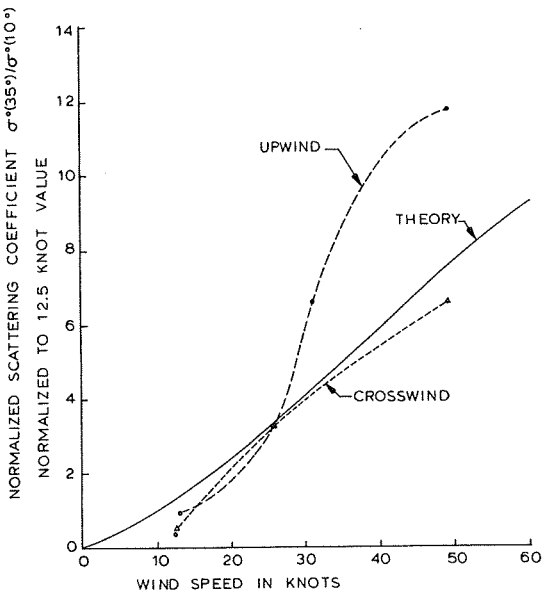

Fig. 11 Comparison of composite-spectrum theory with NASA experimental data. Absolute levels adjusted for coincidence at 25 knots

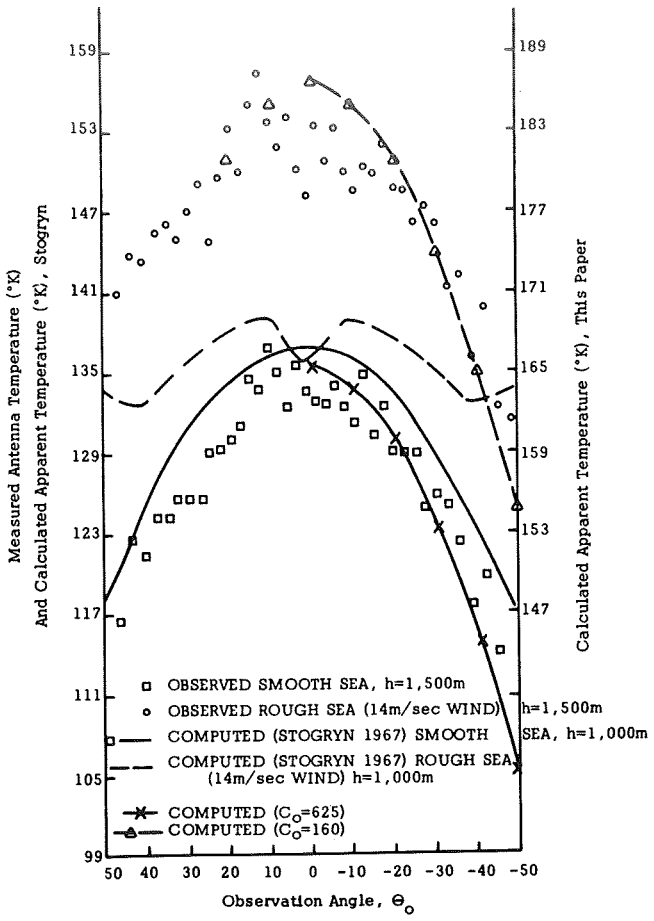

Fig. 12 Measured and calculated horizontally polarized apparent temperature of the ocean at 19.4 GHz. (From Fung and Ulaby, 1970)

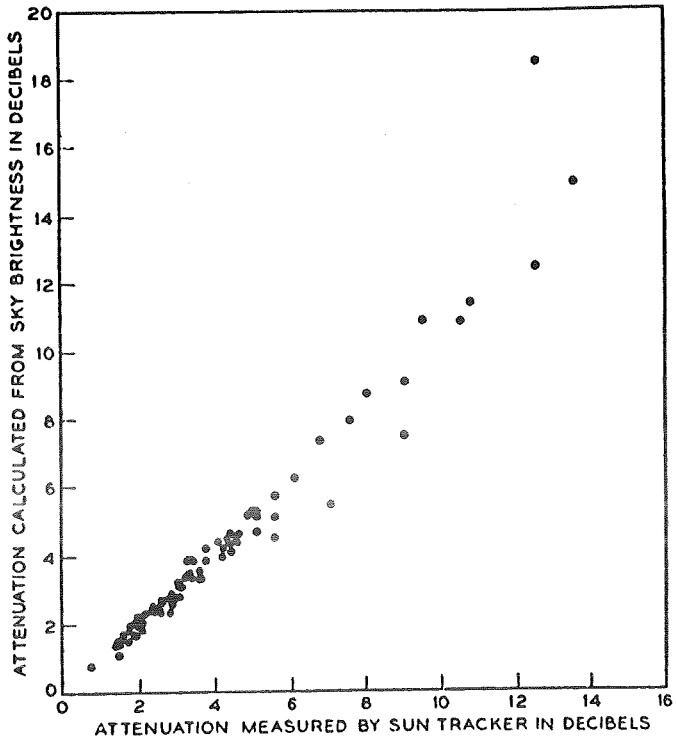

Fig. 13 Comparison of measured attenuation with values calculated from upward-looking microwave radiometer (16 GHz) (from Wilson, 1969)

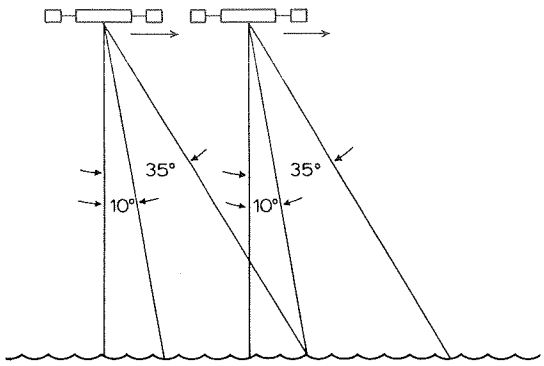

Fig. 14 Satellite mounted scatterometer for sea-state measurements

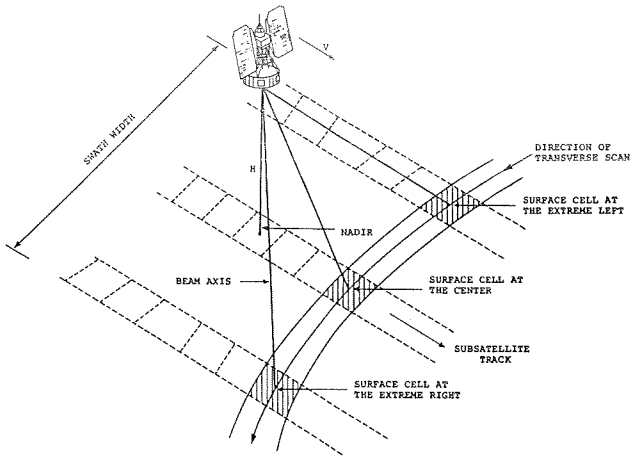

Fig. 15 Scan for an operational radiometer-scatterometer for sea-state measurement

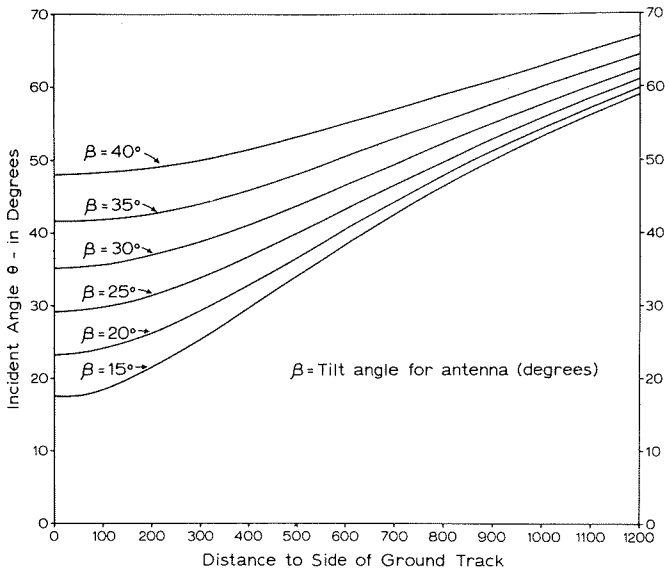

Fig. 16 Incident angle at the earth for a wave from a scanning antenna on a 1000 km altitude satellite

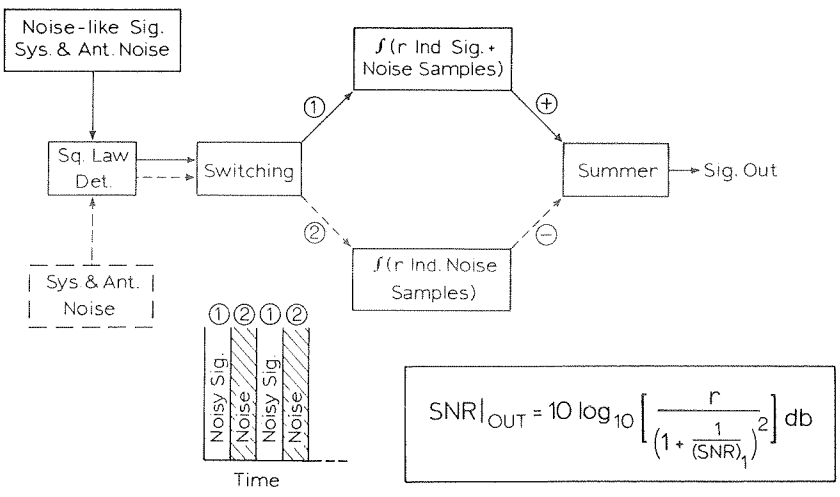

Fig. 17 S/N enhancement scheme for noise-like signals

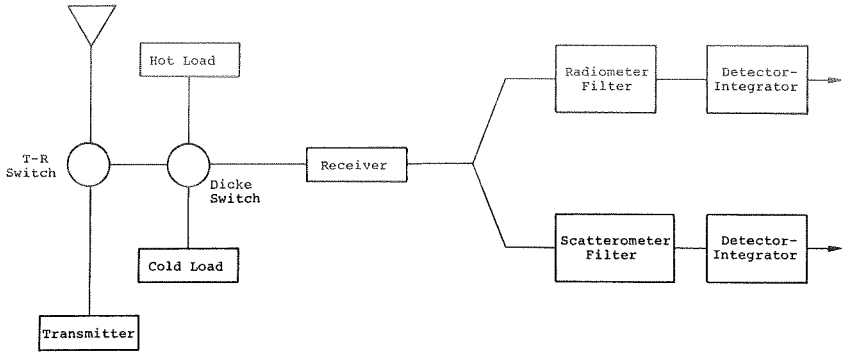

Fig. 18 Elements of a radiometer-scatterometer

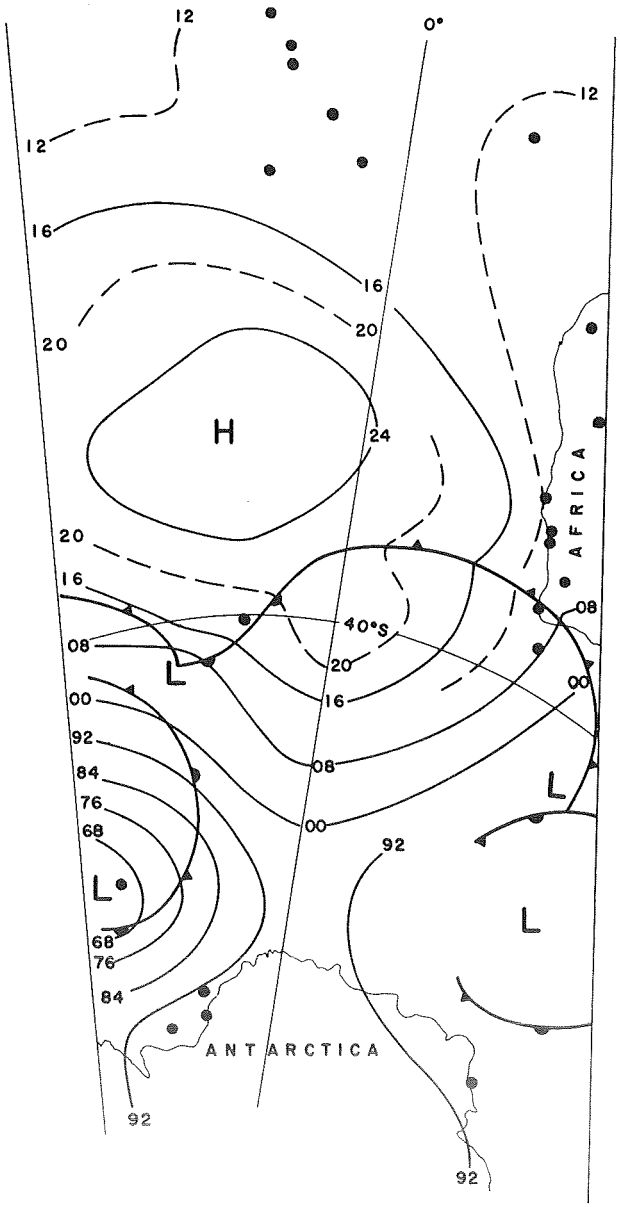

Fig. 19 Portion of the national meteorological center southern hemisphere surface analysis for January 18, 1968. The dots represent points where surface reports were available for the analysis. The analysis is based on these surface points, the southern hemisphere cloud mosaic patterns prepared by ESSA, and continuity considerations

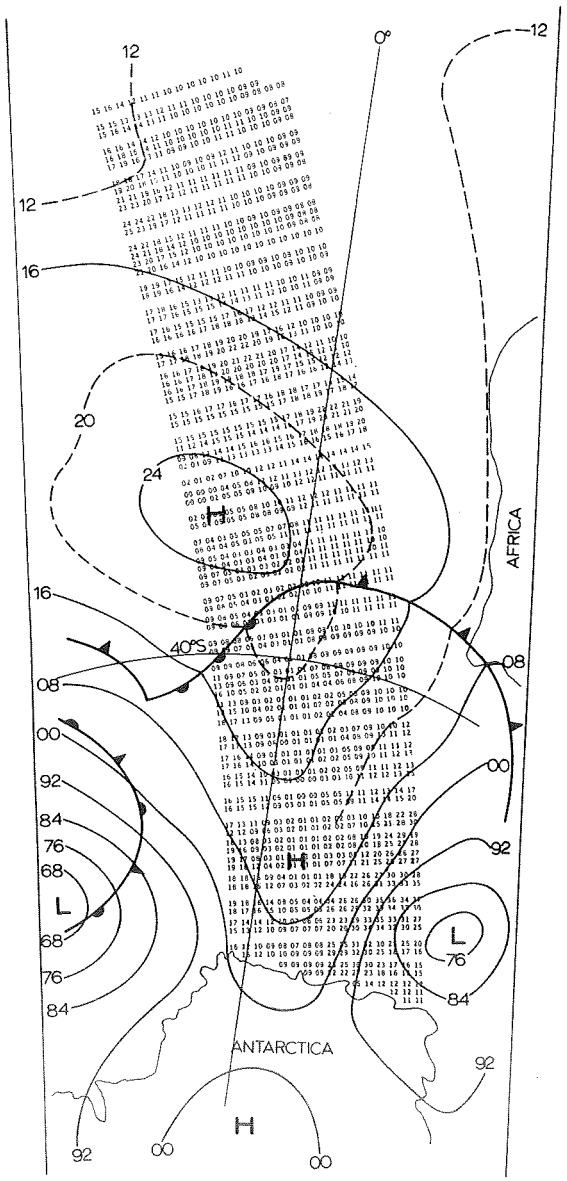

Fig. 20 Hypothetical data that might be obtained from one portion of one pass of a NIMBUS spacecraft with a scatterometer and dual antenna system. The numbers represent the wind speed in knots on a grid that approximates the actual coverage